Cheater-mediated evolution shifts phenotypic heterogeneity in *Bacillus subtilis* biofilms

Marivic Martin[1,2], Anna Dragoš[1], Daniel Schäfer[2], Gergely Maróti[3], and Ákos T. Kovács[1,2]

[1] Bacterial Interactions and Evolution Group, Technical University of Denmark, 2800 Kongens Lyngby, Denmark

[2] Terrestrial Biofilms Group, Friedrich Schiller University Jena, 07743 Jena, Germany

[3] Institute of Plant Biology, Biological Research Center of the Hungarian Academy of Sciences, 3600 Szeged, Hungary

Corresponding Author: Ákos T. Kovács

Bacterial Interactions and Evolution Group, Technical University of Denmark, 2800 Kongens Lyngby, Denmark; atkovacs@dtu.dk; +45 45252527

Keywords: *Bacillus subtilis*, biofilm, phenotypic heterogeneity, experimental evolution, exopolysaccharide

ABSTRACT

Biofilms are closely packed cells held and shielded by extracellular matrix composed of structural proteins and exopolysaccharides (EPS). As matrix components are costly to produce and shared within the population, EPS-deficient cells can act as cheaters by gaining benefits from the cooperative nature of EPS producers. Remarkably, genetically programmed EPS producers can also exhibit phenotypic heterogeneity at single cell level. For instance, mature biofilms of *Bacillus subtilis* contain cells in an 'ON' state, expressing extracellular matrix genes, as well as cells in an 'OFF' state. Previous studies have shown that spatial structure of biofilms limits the spread of cheaters, but the long-term influence of cheating on biofilm evolution is not well understood. In addition, the influence of cheats on phenotypic heterogeneity pattern within matrix-producers, was never examined. Here, we describe the long-term dynamics between EPS producers (cooperators) and non-producers (cheaters) in *B. subtilis* biofilms and track changes in phenotypic heterogeneity of matrix production within the populations of co-operators. We discovered that cheater-mediated evolution in pellicles leads to a transient shift in phenotypic heterogeneity pattern of co-operators, namely an increased number of *eps* expressing cells as depicted by hyper ON phenotype. Although hyper ON strategy seems adaptive in presence of cheats, it is soon substituted by hyper OFF phenotype and/or soon after by population collapse. This study provides additional insights on how biofilms adapt and respond to stress caused by exploitation in long-term scenario.

SIGNIFICANCE STATEMENT

Microbial biofilms are significant in medical, environmental and industrial settings. Biofilm control strategies have been proven to be challenging due to their increased resistance to antimicrobials. Here, we employ a cheater-mediated evolution study in *Bacillus subtilis* pellicles to understand in long-term scale how biofilms' social behavior evolves as triggered by stress. We show that evolution of matrix-producing cells (cooperators) in the presence of non-producers

(cheaters) leads to a cheating strategy that allows cheaters to benefit from cooperators, that subsequently result to population tragedy. However, cooperators can also adapt and evade exploitation via an anti-cheating system that involves shift in phenotypic heterogeneity related to biofilm matrix expression. This study highlights biofilm adaptation and stress response mechanisms within the context of evolution.

INTRODUCTION

Cooperative interactions are prevalent for all life forms (1), even for simple microbes that often exist in communities of matrix bound surface-attached cells called biofilms (2–6). However, when costly products such as siderophores (7, 8), extracellular polymeric substances (9, 10), digestive enzymes (11), and signaling molecules (12, 13) are secreted and shared, cooperative behavior becomes susceptible to cheating (2, 14–16), where mutants defective in cooperation can still benefit from cooperative community members (4, 5, 17). It has been shown that spatially structured biofilms, where interactions with clonemates are common and diffusion of public goods is limited, may serve as natural defense against cheating (18–20). However, long time scale studies have recently reported that biofilm defectors can spontaneously emerge and spread in biofilms by exploiting other matrix-proficient lineages (21–24). In fact, a pioneering microbial evolution study on *Pseudomonas fluorescens* has already pointed towards dynamic evolutionary interplay between cooperation and exploitation in biofilm matts (25), where emergence of cellulose overproducer (Wrinkly) allowed matt formation, but also created an opportunity for exploitation by non-producers (Smooth), eventually leading to so called 'tragedy of the commons' (4, 26, 27).

Taken together, biofilms are suitable model to understand social interactions in an evolutionary time scale (23, 28–31). Modelling and empirical data confirm that mutualism (beneficial to both actor and recipient) and altruism (beneficial to recipient but not to actor) play crucial role in biofilm enhancement (32) but at the same time can lead to biofilm destabilization (25). Can

71 cooperators evolve tactics to evade exploitation and in turn, can cheats utilize evolution to
72 enhance their selfish actions?
73 Recent studies showed that in well-mixed environment, cooperators adapt to cheats by reducing
74 cooperation (14, 15, 33). Such reduction could be achieved by various strategies, for instance
75 decrease in motility (15), down regulation or minimal production in public goods (14, 15, 33), up-
76 regulation of other alternative public goods (14), or bi-stable expression in virulence gene (2).
77 Interestingly, populations of cooperators often exhibit phenotypic heterogeneity at the single
78 cell level (34, 35). Therefore, an alternative and simple mechanism to modulate levels of
79 cooperation in a population, would be through changes in phenotypic heterogeneity pattern.
80 However, the long-term effects of cheats on costly goods' expression at individual cell level have
81 never been examined. Understanding how heterogeneity of gene expression within the
82 population is affected in the presence of cheats would provide better insight on microbial
83 adaptation and stress response mechanisms.
84 Here, we address this question using pellicle biofilm model of *Bacillus subtilis.* Pellicle formation
85 in *B. subtilis* involves, amongst others, aerotaxis driven motility and subsequent matrix
86 production (36). Aerotaxis is important for oxygen sensing to aid cells reach the surface, while
87 matrix formation is significant to sustain cells to adhere to the surface and to each other.
88 Exopolysaccharide (EPS) is a costly public good in *Bacillus subtilis* biofilms (10, 18, 37) and is
89 heterogeneously expressed during biofilm formation with approximately 40% of cells exhibiting
90 the ON state (37, 38). We aimed to investigate the long-term dynamics between EPS producer
91 (cooperator) and EPS deficient (cheater) cells and assess cheat-dependent alteration related to
92 phenotypic heterogeneity in *eps* expression by the producer.
93 We reveal, that initial cheating mitigation by the EPS producers involves shift in phenotypic
94 heterogeneity towards increased frequency of *eps*-expressing cells, which is achieved by loss-of-
95 function mutation in a single regulatory gene. We also demonstrate, that although 'hyper ON'
96 phenotype helps to reduce cheating, it is rapidly replaced by hyper OFF strategy, which,

97 combined with certain mutations in EPS deficient strain, results in tragedy of the commons and
98 population collapse. Our study uncovers an alternative anti-cheating mechanism based on
99 changes in phenotypic heterogeneity and highlights meandering trajectories prior cooperation
100 collapse.
101
102 **RESULTS**
103
104 **Long-term cheating in pellicle biofilms leads to population collapse**
105 Exopolysaccharide EPS is one of the major components of *B. subtilis* biofilm matrix and mutants
106 deficient in EPS production (Δ*eps*) are not able to form pellicle biofilms (*SI Appendix*, Fig. S1A and
107 S1B). Since it was previously demonstrated that EPS can be shared (10, 18, 37), we predicted that
108 Δ*eps* would be able to take advantage of EPS-producing wild type (WT) and incorporate into the
109 pellicle biofilm. Indeed, when co-cultivated with the WT (at 1:1 initial ratio), the Δ*eps* became
110 part of the pellicle with negative impact on WT productivity (*SI Appendix*, Fig. S1b). In addition,
111 presence of the mutant resulted in decreased level of surface complexity as typical wrinkly
112 structures were absent in the mixed pellicle (*SI Appendix*, Fig. S1a). These results reveal that the
113 Δ*eps* serves as cheater in the pellicle biofilms by taking advantage of the EPS producer strain.
114 In order to examine long-term population dynamics in co-culture of EPS producers (wild type-
115 WT) and cheats (Δ*eps*), we allowed 8 parallel pellicle populations of Δ*eps*+WT to evolve for 35
116 cycles (~200 generations) starting at 1:1 initial ratio. Every 5th transfer, we determined relative
117 frequencies (%) of both strains in the pellicles using plate count assay (CFU/ml). The results
118 revealed that cheats were able to outnumber the producer strain, eventually leading to
119 decreased productivity of the entire population, as pellicle formation was no longer possible
120 (Fig. 1). Such scenario was observed in 6 out of 8 populations and will be referred to as
121 population collapse (Fig. 1). Evolutionary time points when a collapse occurred varied among
122 the population, for instance in population 1 and 7, the collapse was observed after 30th transfer

123 while in population 2 it took place already after 10th transfer. No collapse was observed for
124 populations 5 and 8, where cheats coexisted with WT until the end of the evolution cycle (35th).
125 We also observed different patterns of how productivity of the WT changed when evolved in
126 the presence of cheats (Fig. 1). A "decline-collapse" trend was noticed for populations 2, 3 and
127 4, wherein the WT continuously declined and then proceeded to population collapse after 5th,
128 15th and 10th transfers, respectively. For populations 1, 6 and 7, we witnessed a "decline-
129 recovery-collapse" pattern. Finally, we detected a "decline-recovery-no collapse" model for
130 populations 5 and 8, wherein the populations after recovering from an early decline persisted
131 until 35th transfer.
132
133 **'Hyper ON' matrix producers emerge during evolution with cheats**
134 Previous studies have shown that cooperators can adapt to presence of cheats for example by
135 decreasing the amount of released public goods and therefore minimizing cheating opportunities
136 (2, 14, 15). As *B. subtilis* exhibits phenotypic heterogeneity in *eps* matrix gene expression (37, 38)
137 (*SI Appendix*, Fig. S2), we investigated how such heterogeneous expression is influenced by the
138 presence of cheats in an evolutionary perspective. Using confocal laser scanning microscopy,
139 qualitative assessment of randomly selected isolates revealed that early populations of the EPS
140 producers (5-10 transfer) which co-evolved with cheats exhibited a so called hyper ON
141 phenotype, where the fraction of *eps* expressing cells was largely increased as compared to the
142 ancestral strain (*SI Appendix*, Fig. S2). On the contrary, evolution in the absence of Δ*eps* mostly
143 resulted in hyper OFF phenotype, with larger amounts of cells that do not express *eps*. To further
144 verify this phenomenon, we quantified the average P_{eps}-GFP intensity of 95 single isolates per
145 each WT population (see methods) (Fig. 2). The results revealed major changes in distribution of
146 P_{eps}-GFP intensity across the evolved and co-evolved WT populations as compared to the WT
147 ancestor (Fig. 2). Specifically, for all WTs evolved alone, the distributions narrowed and
148 dramatically shifted to the left, so that the clear majority of isolates matched the hyper OFF

149 category across the entire evolutionary time (5-35th transfer) (Fig. 2.). On the contrary, in some
150 co-evolved WT populations (population 3, 5 and 7) the distributions widened at the 10th transfer
151 (Fig. 2), resulting in increased frequency of hyper ON isolates (Fig. 2). A transient increase of
152 hyper ON phenotype frequency appeared rather temporary, as it was followed by dramatic
153 increase in frequency of hyper OFF phenotype in later evolutionary time points (Fig. 2.).
154

155 **Mutations in *rsiX* lead to Hyper ON phenotype**

156 To unravel the genetic basis of the hyper ON phenotype that evolved in presence of cheats,
157 several single isolates from the evolved populations were subjected to genome resequencing
158 (for details see methods). The comparative analysis of sequencing data revealed that the WT
159 isolates that co-evolved with cheats and exhibited the hyper ON phenotype, shared mutations
160 in *rsiX* gene (*SI Appendix*, Dataset S1). The *rsiX* gene encodes for an anti-sigma factor that controls
161 the activity of extracellular cytoplasmic function (ECF) sigma factor X which is involved in cationic
162 antimicrobial peptide resistance important for cell envelope stress response (39). Detected
163 mutations resulted either in substitution of Valine 106 to Alanine or frameshift mutations in
164 Serine 104 or Isoleucine 347 that could lead to change or loss of anti-SigX function. Indeed, we
165 were able to recreate the evolved hyper ON phenotype in the pellicle solely by deleting the *rsiX*
166 gene in the WT ancestor (Fig. 3C). Interestingly, a different type of frameshift mutation in Lysine
167 200 was found in one population of evolved WT alone but this population demonstrated a hyper
168 OFF phenotype (Fig. 3A), suggesting that only certain types of mutations in *rsiX* lead to the
169 increase in number of *eps* expressing cells in the population or additional mutations have
170 antagonistic effects in this isolate.
171

172 **Mutation in *rsiX* contributes to competitive advantage of producer strains against cheats**

173 As mutation in *rsiX* resulted in hyper ON phenotype that may be linked to elevated secretion of
174 EPS, we hypothesized that Δ*rsiX* producers could support the spread of cheats and contribute to

175 population collapse scenario (Fig.1). To better understand how ancestor WT and Δ*rsiX* interact
176 with Δ*eps,* we cultivated the Δ*eps* in presence of EPS-containing supernatants obtained from the
177 WT and Δ*rsiX* (*SI Appendix*, Fig. S4). Both supernatants could partially restore pellicle formation
178 by Δ*eps* resulting in similar productivities of Δ*eps,* thereby not supporting our hypothesis on
179 improved performance of the mutant in presence of hyper ON Δ*rsiX* strain.
180 In order to determine the effect of *rsiX* deletion on fitness of the WT in presence of cheats, we
181 performed a series of competition assays. Apparently, the Δ*rsiX* showed two-fold increase in
182 relative frequency (40%) (Fig. 4 and *SI Appendix*, Fig. S5) when competed against the Δ*eps*, as
183 compared to the WT ancestor (20%).
184 It is worth to mention that we could not detect any significant fitness costs or benefits linked to
185 *rsiX* deletion in pairwise competition between Δ*rsiX* and WT (*SI Appendix*, Fig. S5; relative fitness
186 of Δ*rsiX* = 1.00 ±0.02 S.D.). Furthermore, we did not observe significant differences in
187 productivities of WT and the hyper ON Δ*rsiX* mutant, when grown in monoculture pellicles (*SI*
188 *Appendix*, Fig. S3), suggesting that positive effect of *rsiX* mutation only manifests in presence of
189 cheats.
190 Relative frequencies of the evolved WT strains carrying hyper ON phenotype and specific
191 mutations in *rsiX* were even higher (average ranged from 58% to 99%) as compared to Δ*rsiX*
192 carrying ancestral genetic background (Fig. 4, Fig. S6). Remarkably, the significant fitness
193 improvement of the WT evolved with cheats was already observed in 5th transfer and 10th
194 transfer, mutually with an early occurrence of hyper ON phenotype in those populations. This
195 was not the case for the WT evolved alone at 5th transfer (20%), where a remarkable fitness
196 increase (average ranged from 87% to 94%) could only be observed in later evolutionary time
197 point (Fig. 4 and *SI Appendix*, Fig. S6). These results suggest that the early improvement in
198 competitive strategies against cheats are caused by the *rsiX* mutation and other mutations
199 associated with hyper ON phenotype, while in later evolutionary time points this effect can be
200 amplified by cheating-independent adaptation to the medium. Interestingly, frequencies of Δ*eps*

201 in pellicles formed by the ancestor or evolved matrix producers, did not manifest in productivity
202 assay (Fig. 4b). These suggests that hyper ON phenotypes are vested on the increase in *eps*-
203 expressing cells or limiting the spread of cheats but do not result in an increase in total yield.
204

205 **_sinR_ mutation negatively affects the competitive advantage of cheats**

206 Interestingly, evolved cheaters that were isolated from the same populations as *rsiX* mutation
207 containing matrix producers (i.e. populations 3 at 5th and 10th transfers and 7 at 10th and 30th
208 transfers), harbored a *sinR* mutation of an amino acid substitution from Leucine 1 to Tryptophan
209 (*SI Appendix*, Dataset S1). Therefore, we anticipated that the mutation may influence
210 competitive fitness of the Δ*eps* against the WT matrix producer. The *sinR* gene encodes for a
211 transcriptional repressor and biofilm master regulator that controls the operons e*psA-O* and
212 *tapA-sipW-tasA* for matrix exopolysaccharide and protein component, respectively (40).
213 Interestingly, our results showed that the evolved Δ*eps* with an ancestor *sinR* (Δ*eps* $sinR^{WT}$)
214 performed better against the WT ancestor as compared to evolved Δ*eps* that carried *sinR*
215 mutation (Δ*eps* $sinR^{Leu1Trp}$) (Fig. 5 and *SI Appendix*, Fig. S7), suggesting that mutation in *sinR* could
216 prevent the spread of cheats in the evolved populations, especially at early stage of co-evolution
217 (Fig. 4 and *SI Appendix*, Fig. S6). Interestingly, the impact of *sinR* mutation in Δ*eps* is nearly lost
218 when WT carries *rsiX* deletion or other adaptive mutations (Fig. 5 and *SI Appendix*, Fig. S7, S8).
219

220 **Population collapse may be linked to adaptive mutations in cheats and loss of _rsiX_ mutants in**
221 **producer populations**

222 To explore possible reasons behind the collapse of certain WT vs Δ*eps* populations, the co-
223 evolved populations of WTs and Δ*eps* were isolated from selected co-cultures stocks (see
224 methods) at final evolutionary timepoint (populations 5 and 8) or at last time point prior to
225 collapse (populations 4 and 6) and subjected to whole genome re-sequencing. Genomic analysis
226 of Δ*eps* populations that caused early pellicle collapse (pop 4 and 6) revealed several mutations

227 in chemo/aerotaxis genes, namely in *hemAT* (Fig. 6 and *SI Appendix*, Dataset S2) with amino acid
228 change from Glutamic acid 254 to Lysine and Lysine 131 to Threonine for populations 6 and 4,
229 respectively. Interestingly, we did not identify any genetic changes in WT from population 4,
230 suggesting that the collapse was triggered by adaptation of the Δ*eps.* On the other hand, for the
231 non-collapsed populations (population 5 and 8) the consensus could be observed in the WTs,
232 which showed mutations in *yvrG* gene (Fig. 6 and *SI Appendix*, Dataset S2) encoding for two-
233 component histidine kinase involved in cell wall process. Finally, *rsiX* mutation was not detected
234 neither in the last populations before collapse, with an exemption of population 7 with 1% hyper
235 ON phenotype (Fig. 2, 6 and *SI Appendix*, Dataset S1), nor at the last transfer point for the non-
236 collapse, implying that this mutation was lost in parallel with the loss of hyper ON phenotype in
237 the late populations.
238
239 **DISCUSSION**
240 Studies on evolution of cooperative behavior is important to understand how social behaviors
241 are shaped in longer time scale. Moreover, exploring long term consequences of exposure to
242 cheating allows to better understand how cooperation prevails in nature where environmental
243 stress and exploitation exist inherently. Previous evolution studies on cheater-cooperator
244 interactions in spatially structured environment showed cheater mitigation via minimization of
245 the cooperative trait (2, 14, 15). On the contrary, here we show that cooperators initially respond
246 to cheating by intensifying the cooperative behaviors through shift in phenotypic heterogeneity
247 pattern towards hyper ON phenotype, where, in contrast to the ancestral strain, nearly all
248 members of the population express the operon involved EPS production. Further molecular
249 analysis of the hyper ON isolates strongly suggests that this phenotype is triggered by loss-of-
250 function mutation in *rsiX* gene. The product of *rsiX* represses the activity of ECF sigma factor, SigX
251 that is involved cell envelope stress response against cationic antimicrobial peptides (41).
252 Importantly, SigX has been previously shown to induce expression of *epsA-O* in B. subtilis via a

253 complex regulatory pathway involving Abh and SlrR (42), explaining the observed enhanced in
254 *eps* gene expression in *rsiX* mutant. Another example of matrix overproduction via ECF
255 adaptation was also reported in Gram-negative bacterium *Pseudomonas aeruginosa* where
256 mutations in another ECF called AlgT led to alginate overproduction and increased resistance to
257 antimicrobials (43). Therefore, adaptive boosts in matrix production through modulation of ECF
258 is not exclusive for *B. subtilis* but seems to occur also in medically relevant Gram-negative
259 pathogens like *P. aeruginosa*.
260 Interestingly, we also observed that *rsiX* mutation carrying matrix producers tend to co-occur
261 with $sinR^{Leu1Trp}$ cheaters (Δ*eps*) (Fig. 6 *SI Appendix*, Dataset S1). SinR is a transcriptional repressor
262 and master regulator of biofilm (40) and changes in the N terminal of SinR reveal big impact on
263 its functions (44), we expect that alterations in the first amino acid could provide immense effect
264 either on translation rate, folding stability or function. We have previously observed that loss-of-
265 function mutation in Δ*eps* enhances the production of TasA, a protein constituent which is
266 another essential matrix component (37). Furthermore, biofilm productivity can be maximized
267 by division of labor between TasA- and EPS-producers (37). We hypothesize that similar
268 phenomenon might transiently improve productivity of mixed pellicles, where cooperators
269 overproduced EPS while cheaters overproduced TasA. Alternatively, as TasA carries antimicrobial
270 properties (45, 46), its increased abundance could trigger stress response in the co-operator,
271 selecting for *rsiX* mutation. This could explain the synchronous appearance of *rsiX* mutations with
272 hyper ON phenotypes in evolved cooperators and *sinR* mutations in evolved cheaters.
273 In contrast to previous studies, that addressed long term cheating on diffusible siderophores, we
274 explored evolutionary interplay between biofilm producers and non-producers in structured
275 environment. Our results support previous observations on evolution of specific cheating-
276 resisting mechanisms in co-operators, pointing towards ubiquity of this phenomenon. In
277 addition, our work brings up two major findings 1) matrix producers can adapt to matrix non-
278 producers by shifting phenotypic heterogeneity towards increased number of matrix-expressing

279 cells 2) hyper ON anti-cheating strategy is a short-term solution, which can either be replaced by
280 another, yet unknown strategy linked to hyper OFF phenotype, or followed by tragedy of the
281 commons. As recently demonstrated, alternative EPS-independent biofilm formation strategies
282 can emerge by single amino acid change is TasA (47). It remains to be discovered whether shifts
283 in phenotypic heterogeneity in response to long term cheating is general phenomenon that
284 applies to different types of public goods.
285

286 **MATERIALS AND METHODS**

287 **Bacterial strains and culture conditions**

288 Strain *B. subtilis* 168 $P_{hyperspank}$-mKATE P_{eps}-GFP (TB869) was obtained by transforming the
289 laboratory strain, *B. subtilis* 168 $P_{hyperspank}$-mKATE (TB49) (10, 18), with genomic DNA from
290 NRS2243 (*sacA*::P_{epsA}-*gfp*(Km)*hag*::cat) and selecting for Km resistance. The Δ*rsiX* strain with
291 fluorescence reporters (TB959) was obtained by transforming TB869 with genomic DNA isolated
292 from BKE23090 (168 *trpC*2 Δ*rsiX*::erm) (48). Strains were maintained in LB medium (Lysogeny
293 Broth (Lennox), Carl Roth, Germany), while 2×SG medium was used for biofilm induction (10).
294 The Δ*eps* strains (TB608) was created previously (10).
295

296 **Experimental evolution**

297 Eight biological replicates of the co-cultures of 1:1 ratio of *B. subtilis* TB869 and TB608 were
298 grown in 48-well plate containing 1ml 2×SG medium at 30°C for two days. Pellicles were
299 harvested into Eppendorf tubes containing 500 μl sterile 2×SG medium and 100 μl of sterile glass
300 sand, vortexed for 90 seconds, 10 μl fraction was transferred into 1ml 2×SG medium of a 48 well
301 plate, and incubated at 30°C static condition for two days. This cycle was continuously repeated
302 35 times. As control, four biological replicates of mono-cultures of *B. subtilis* TB869 were evolved
303 using the same transfer method. Every 5th transfer cycle, harvested cultures were mixed with
304 15% glycerol and stored at –80°C.

305

306 **Population ratio assay**

307 At every 5th transfer, pellicle biofilm productivities and relative frequencies of mutants and WT
308 were qualitatively assessed (colony forming units (CFU)/ml) using LB agar containing selective
309 antibiotics. LB agar plates were incubated at 37°C for 16 hours and colonies were counted. Three
310 single clones of WT and of *Δeps* per population per timepoint were isolated from plates and
311 stored at –80°C in the presence of 15% glycerol.

312

313 **Quantitative assessment of hyper ON and hyper OFF populations**

314 Ninety-five single isolates of ancestor or evolved TB869 strains obtained from the population per
315 timepoint were allowed to form pellicles in 96-well PCR plate containing 100µl 2×SG medium.
316 After incubation at 30°C for 24 hours, the plate was vortexed for 90 seconds, bath sonicated
317 (mini ultrasonic bath, Carl Roth, Germany) for 5 minutes and fluorescence was recorded using
318 TECAN Infinite F200 PRO microplate reader (excitation at 485/20 nm and emission at 535/10 nm
319 for GFP; excitation at 590/20 nm and emission at 635/35 nm for RFP; using manual gain of 35
320 and 50 for GFP and RFP, respectively). Hyper ON and hyper OFF phenotypes were categorized
321 based on cut off value of the WT ancestor mean ± 1SD. GFP intensity values above 134 arbitrary
322 units (AU) were considered as hyper ON and values below 70 AU were categorized as hyper OFF.

323

324 **Pellicle competition assay**

325 Pellicles grown from 1:1 ratio of competing strains and incubated for two days were subjected
326 to competition assay as previously described (10).

327

328 **Qualitative assessment of Hyper ONs and Hyper OFFs via microscopy**

329 Single clones of WT obtained from population ratio assay were allowed to form 1-day old pellicle.
330 Harvested pellicles were subjected to microscopic analysis using an Axio Observer 780 Laser

331 Scanning Confocal Microscope (Carl Zeiss) equipped with a Plan-Apochromat 63×/1.4 Oil DIC
332 M27 objective, an argon laser for stimulation of fluorescence (excitation at 488 for green
333 fluorescence and 561 nm for red fluorescence, with emission at 528/26 nm and 630/32 nm
334 respectively). Zen 2012 Software (Carl Zeiss) and FIJI Image J Software (49) were used for image
335 recording and processing, respectively.
336

337 **Genome re-sequencing and genome analysis**

338 Genomic DNA of single clones from selected evolved populations were isolated using Bacterial
339 and Yeast Genomic DNA kit (EURx) directly from –80°C stocks grown in LB medium for 5 hours at
340 37°C with shaking at 220 rpm. For population sequencing analysis, approx. 100 colonies
341 belonging to the evolved populations were harvested into 2ml LB broth and incubated at 37°C
342 shaking at 220 rpm for 2-3 hours. Re-sequencing was performed on an Illumina NextSeq
343 instrument using V2 sequencing chemistry (2x150 nt). Base-calling was carried out with
344 "bcl2fastq" software (v.2.17.1.14, Illumina). Paired-end reads were further analyzed in CLC
345 Genomics Workbench Tool 9.5.1. Reads were quality-trimmed using an error probability of 0.05
346 (Q13) as the threshold. Reads that displayed ≥80% similarity to the reference over ≥80% of their
347 read lengths were used in mapping. Quality-based SNP and small In/Del variant calling was
348 carried out requiring ≥10× read coverage with ≥25% variant frequency. Only variants supported
349 by good quality bases (Q ≥ 30) on both strands were considered. Gene functions (product names)
350 in *SI Appendix* Datasets were reported based on SubtiWiki (50).
351

352 **Acknowledgements**

353 This work was funded by the Deutsche Forschungsgemeinschaft (DFG) to Á.T.K. (KO4741/2.1)
354 within the Priority Program SPP1617. M.M. was supported a FEMS Research and Training Grant
355 (FEMS-RG-2017-0054). A.D. has received funding from the European Union's Horizon 2020
356 research and innovation programme under the Marie Sklodowska-Curie grant agreement no.

713683 (H.C. Ørsted COFUND). Work in the laboratory of Á.T.K. is supported by a DTU startup fund and partly by the Danish National Research Foundation (DNRF137) for the Center for Microbial Secondary Metabolites.

Authors contributions

Á.T.K. conceived the project, M.M., A.D., and D.S. performed the experiments. G.M contributed with methods. M.M., A.D. and Á.T.K. wrote the manuscript, with all authors contributing to the final version.

365 **REFERENCES**

366 1. Bourke A (2011) *Principals of social evolution: Oxford series in ecology and evolution.*
367 (Oxford University Press, Oxford, UK).
368 2. Diard M, et al. (2013) Stabilization of cooperative virulence by the expression of an
369 avirulent phenotype. *Nature* 494:353–356.
370 3. Nadell CD, Xavier JB, Foster KR (2009) The sociobiology of biofilms. *FEMS Microbiol Rev*
371 33:206–224.
372 4. West SA, Diggle SP, Buckling A, Gardner A, Griffin AS (2007) The social lives of microbes.
373 *Annu Rev Ecol Evol Syst* 38:53–77.
374 5. West S a., Griffin AS, Gardner A (2007) Evolutionary explanations for cooperation. *Curr*
375 *Biol* 17:661–672.
376 6. Xavier J, Foster KR (2007) Cooperation and conflict in microbial biofilms. *Proc Natl Adac*
377 *Sci USA* 104:876–881.
378 7. Luján AM, Gómez P, Buckling A (2015) Siderophore cooperation of the bacterium
379 Pseudomonas fluorescens in soil. *Biol Lett* 11:20140934.
380 8. Weigert M, Kümmerli R (2017) The physical boundaries of public goods cooperation
381 between surface-attached bacterial cells. *Proc R Soc B Biol Sci* 284:20170631.
382 9. Dragoš A, Kovács ÁT (2017) The peculiar functions of the bacterial extracellular matrix.
383 *Trends Microbiol* 25:257–266.
384 10. Martin M, et al. (2017) *De novo* evolved interference competition promotes the spread
385 of biofilm defectors. *Nat Commun* 8:15127.
386 11. Folse HJ, Allison SD (2012) Cooperation, competition, and coalitions in enzyme-
387 producing microbes: Social evolution and nutrient depolymerization rates. *Front*
388 *Microbiol* 3:338.
389 12. Popat R, et al. (2012) Quorum-sensing and cheating in bacterial biofilms. *Proc R Soc B*
390 *Biol Sci* 279:4765–4771.

391 13. Dogsa I, Oslizlo A, Stefanic P, Mandic-mulec I (2014) Social interactions and biofilm
392 formation in *Bacillus subtilis*. *Food Technol Biotechnol* 52:149–157.
393 14. O'Brien S, Luján AM, Paterson S, Cant MA, Buckling A (2017) Adaptation to public goods
394 cheats in *Pseudomonas aeruginosa*. *Proc R Soc B Biol Sci* 284:20171089.
395 15. Kümmerli R, et al. (2015) Co-evolutionary dynamics between public good producers and
396 cheats in the bacterium *Pseudomonas aeruginosa*. *J Evol Biol* 28:2264–2274.
397 16. Harrison F (2013) Dynamic social behaviour in a bacterium: *Pseudomonas aeruginosa*
398 partially compensates for siderophore loss to cheats. *J Evol Biol* 26:1370–1378.
399 17. Hamilton WD (1964) The genetical evolution of social behaviour. I. *J Theor Biol* 7(1):1–16.
400 18. van Gestel J, Weissing FJ, Kuipers OP, Kovács ÁT (2014) Density of founder cells affects
401 spatial pattern formation and cooperation in Bacillus subtilis biofilms. *ISME J* 8:2069–
402 2079.
403 19. Nadell CD, Foster KR, Xavier JB (2010) Emergence of spatial structure in cell groups and
404 the evolution of cooperation. *PLoS Comput Biol* 6:e1000716.
405 20. Momeni B, Waite AJ, Shou W (2013) Spatial self-organization favors heterotypic
406 cooperation over cheating. *Elife* 2:e00960.
407 21. Dragoš A, et al. (2018) Evolution of exploitative interactions during diversification in
408 *Bacillus subtilis* biofilms. *FEMS Microbiol Ecol* 94:fix155.
409 22. Ellis CN, Traverse CC, Mayo-Smith L, Buskirk SW, Cooper VS (2015) Character
410 displacement and the evolution of niche complementarity in a model biofilm
411 community. *Evolution (N Y)* 69:283–293.
412 23. Poltak SR, Cooper VS (2011) Ecological succession in long-term experimentally evolved
413 biofilms produces synergistic communities. *ISME J* 5:369–378.
414 24. Goymer P, et al. (2006) Adaptive divergence in experimental populations of
415 Pseudomonas fluorescens. II. Role of the GGDEF regulator WspR in evolution and
416 development of the wrinkly spreader phenotype. *Genetics* 173:515–526.

417 25. Rainey PB, Rainey K (2003) Evolution of cooperation and conflict in experimental
418 bacterial populations. *Nature* 425:72–74.
419 26. West SA, Griffin AS, Gardner A, Diggle SP (2006) Social evolution theory for
420 microorganisms. *Nat Rev Microbiol* 4:597–607.
421 27. Hardin G (1968) The tragedy of the commons. *Science (80-)* 162(June):1243–1248.
422 28. Martin M, Hölscher T, Dragoš A, Cooper VS, Kovács ÁT (2016) Laboratory evolution of
423 microbial interactions in bacterial biofilms. *J Bacteriol* 198:2564–2571.
424 29. Traverse CC, Mayo-Smith LM, Poltak SR, Cooper VS (2013) Tangled bank of
425 experimentally evolved *Burkholderia* biofilms reflects selection during chronic infections.
426 *Proc Natl Acad Sci U S A* 110:E250-9.
427 30. Madsen JS, et al. (2015) Facultative control of matrix production optimizes competitive
428 fitness in *Pseudomonas aeruginosa* PA14 biofilm models. *Appl Environ Microbiol*
429 81:8414–8426.
430 31. Rainey PB, Travisano M (1998) Adaptive radiation in a heterogeneous environment.
431 *Nature* 394:69–72.
432 32. Kreft JU (2004) Biofilms promote altruism. *Microbiology* 150:2751–2760.
433 33. Lyons NA, Kolter R (2018) A single mutation in rapP induces cheating to prevent cheating
434 in Bacillus subtilis by minimizing public good production. *Commun Biol* 1:133.
435 34. Veening JW, et al. (2008) Transient heterogeneity in extracellular protease production by
436 *Bacillus subtilis*. *Mol Syst Biol* 4:1–15.
437 35. Davidson FA, Seon-Yi C, Stanley-Wall NR (2012) Selective heterogeneity in exoprotease
438 production by *Bacillus subtilis*. *PLoS One* 7:e38574.
439 36. Hölscher T, et al. (2015) Motility, chemotaxis and aerotaxis contribute to
440 competitiveness during bacterial pellicle biofilm development. *J Mol Biol* 427:3695–
441 3708.
442 37. Dragoš A, et al. (2018) Division of labor during biofilm matrix production. *Curr Biol*

443 28:1903–1913.

444 38. Chai Y, Chu F, Kolter R, Losick R (2008) Bistability and biofilm Formation in *Bacillus*
445 *subtilis*. *Mol Microbiol* 67:254–263.

446 39. Helmann JD (2016) *Bacillus subtilis* extracytoplasmic function (ECF) sigma factors and
447 defense of the cell envelope. *Curr Opin Microbiol* 30:122–132.

448 40. Chu F, et al. (2004) A master regulator for biofilm formation by Bacillus subtilis. *Mol*
449 *Microbiol* 55(3):739–749.

450 41. Cao M, Helmann JD (2004) The *Bacillus subtilis* extracytoplasmic-function σX factor
451 regulates modification of the cell envelope and resistance to cationic antimicrobial
452 peptides. *J Bacteriol* 186(4):1136–1146.

453 42. Murray EJ, Strauch M a, Stanley-Wall NR (2009) SigmaX is involved in controlling *Bacillus*
454 *subtilis* biofilm architecture through the AbrB homologue Abh. *J Bacteriol* 191:6822–
455 6832.

456 43. Hentzer M, et al. (2001) Alginate overproduction affects Pseudomonas aeruginosa
457 biofilm structure and function. *J Bacteriol* 183(18):5395–401.

458 44. Subramaniam AR, et al. (2013) A serine sensor for multicellularity in a bacterium. *Elife*
459 2013:1–17.

460 45. Stöver AG, Driks A (1999) Secretion, localization, and antibacterial activity of TasA, a
461 *Bacillus subtilis* spore-associated protein. *J Bacteriol* 181:1664–1672.

462 46. Dragoš A, Kovács ÁT, Claessen D (2017) The role of functional amyloids in multicellular
463 growth and development of Gram-positive bacteria. *Biomolecules* 7:60.

464 47. Dragoš A, et al. (2018) Collapse of genetic division of labour and evolution of autonomy
465 in pellicle biofilms. 3:1451–1460.

466 48. Koo BM, et al. (2017) Construction and analysis of two genome-scale deletion libraries
467 for *Bacillus subtilis*. *Cell Syst* 4:291–305.e7.

468 49. Rueden CT, et al. (2017) ImageJ2: ImageJ for the next generation of scientific image data.

469 *BMC Bioinformatics* 18:529.

470 50. Zhu B, Stülke J (2018) SubtiWiki in 2018: From genes and proteins to functional network

471 annotation of the model organism *Bacillus subtilis*. *Nucleic Acids Res* 46:D743–D748.

472

473

474 **Figure legends**

475 **Fig. 1.** Population dynamics over the course of experimental evolution for eight parallel pellicle
476 populations. Productivity (total CFU/ml) and cheater frequency (%) in the pellicle obtained from
477 plate count assay (CFU/ml) for every 5th transfer starting from the initial count prior to incubation
478 until 35 transfers.

479

480 **Fig. 2.** Quantitative assessment of hyper ONs and hyper OFFs present per evolved population.
481 Percentage of isolates >134 AU value expressing high intensity level of P_{eps}-GFP (hyper ON) and
482 low intensity value of < 70 AU (hyper OFF) for WT evolved and non-evolved strains per timepoint
483 from 5th to 35th transfer for all 8 populations evolved with cheaters and 4 populations evolved
484 alone (n=95). Cut off based on the mean ± 1SD of WT ancestor strain taken at six different days
485 (n=336).

486

487 **Fig. 3.** Qualitative assessment of *eps* gene expression based on confocal laser scanning
488 microscopy showing Δ*rsiX* phenotype similar to strains that were co-evolved with cheaters.
489 Pellicles formed by single clones of evolved or *rsiX* mutated TB869 belonging to (A) population
490 C1 evolved alone at 5th, 30th and 35th timepoint showing Hyper OFF phenotype (B) WT ancestor
491 demonstrating heterogeneous expression (C) Δ*rsiX* exhibiting hyper ON phenotype similar to (D)
492 evolved with cheaters Pop 3 (5th and 10th) and Pop 7 (30th) viewed under the confocal laser
493 scanning microscope. Cells constitutively expressing mKATE are represented in magenta and *eps*-
494 expressing cells are shown in green. Scale bar represents 10µm.

495

496 **Fig. 4.** (A) Pellicle competition assay of single clones belonging to producer populations (non-
497 evolved (n=9), Δ*rsiX* (n=8), evolved with (n=4) and without cheaters (n=4)) against Δ*eps* ancestor
498 and (B) corresponding pellicle productivity based on total CFU/ml. Mean is represented in square
499 inside the box plots; whiskers represent the minimum and maximum; single dots represent the

500 individual data points (n); asterisk (*) represents the significant difference from the WT ancestor
501 ANOVA (P value 0.05).
502
503 **Fig. 5**. Pellicle competition assay against evolved cheater with *sinR*^{WT} (left) and *sinR*^{Leu1Trp} (right)
504 (n=4) on single clones of producers (non-evolved, evolved with and without cheaters). Mean is
505 represented in square; whiskers represent the minimum and maximum; single dots represent
506 the individual data points (n); asterisk (*) represents the significant difference ANOVA (P value
507 0.05).
508
509 **Fig. 6.** Figure summary showing the population dynamics based on producer and cheater
510 frequency per population from 5th transfer to 35th transfers for populations evolved with
511 cheaters with collapse (Pop 1, 2, 3, 4, 6 and 7), without collapse (Pop 5 and 8), and populations
512 evolved without cheaters (C1, C2, C3, C4) with indications of phenotypes based on hyper ON,
513 hyper OFF or heterogenous *eps*-expression. Key mutations on single clone level of evolved WT
514 and evolved Δ*eps* or population level are specified. *rsiX** mutation is not similar to mutation
515 observed in strains evolved with cheaters.
516

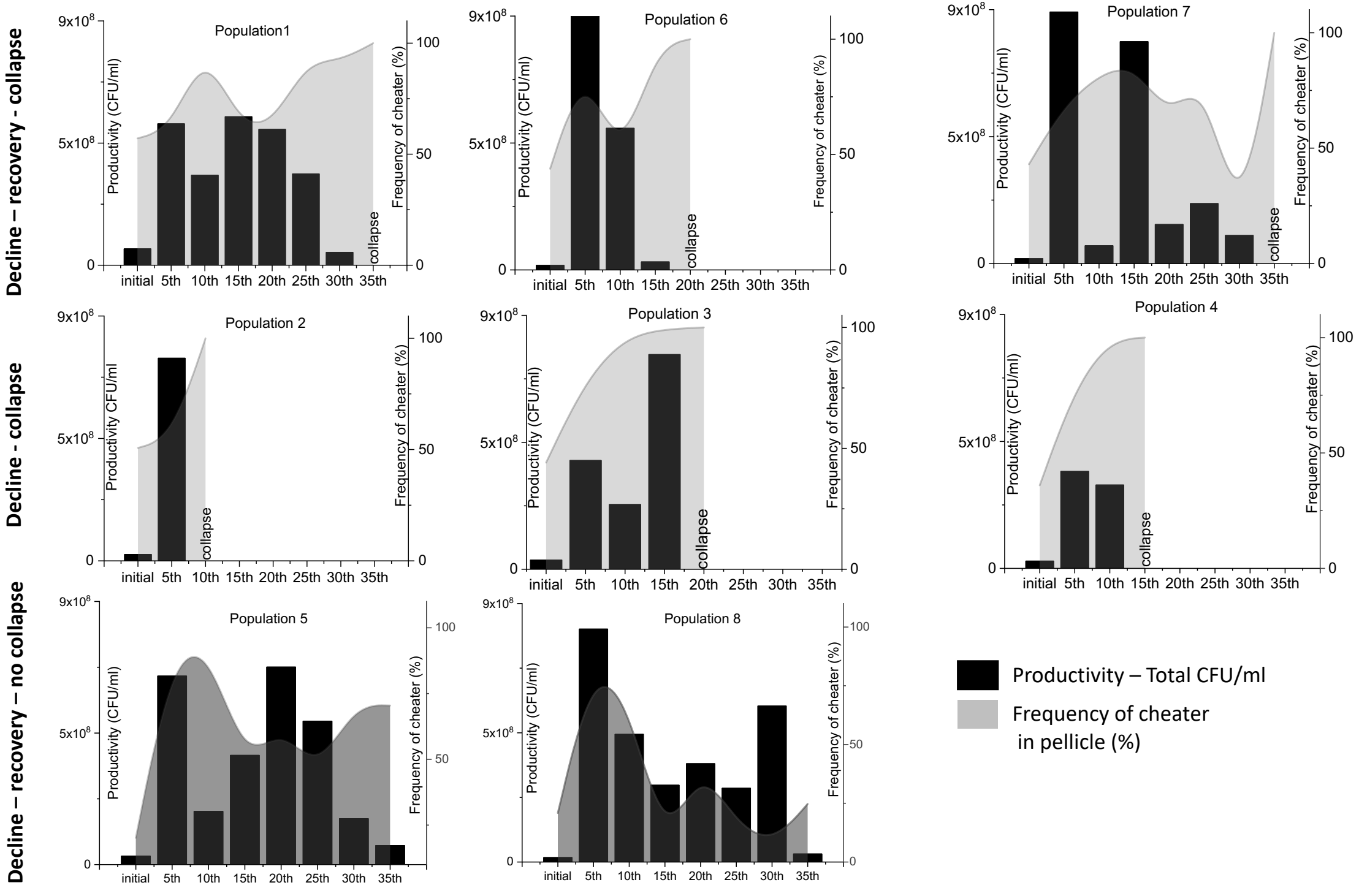
Decline – recovery - collapse
Decline - collapse
Decline – recovery – no collapse
Population1
Population 6
Population 7
Population 2
Population 3
Population 4
Population 5
Population 8
Productivity (CFU/ml)
Productivity CFU/ml
Frequency of cheater (%)
collapse
9x10^8
5x10^8
0
100
50
initial 5th 10th 15th 20th 25th 30th 35th
Productivity – Total CFU/ml
Frequency of cheater in pellicle (%)

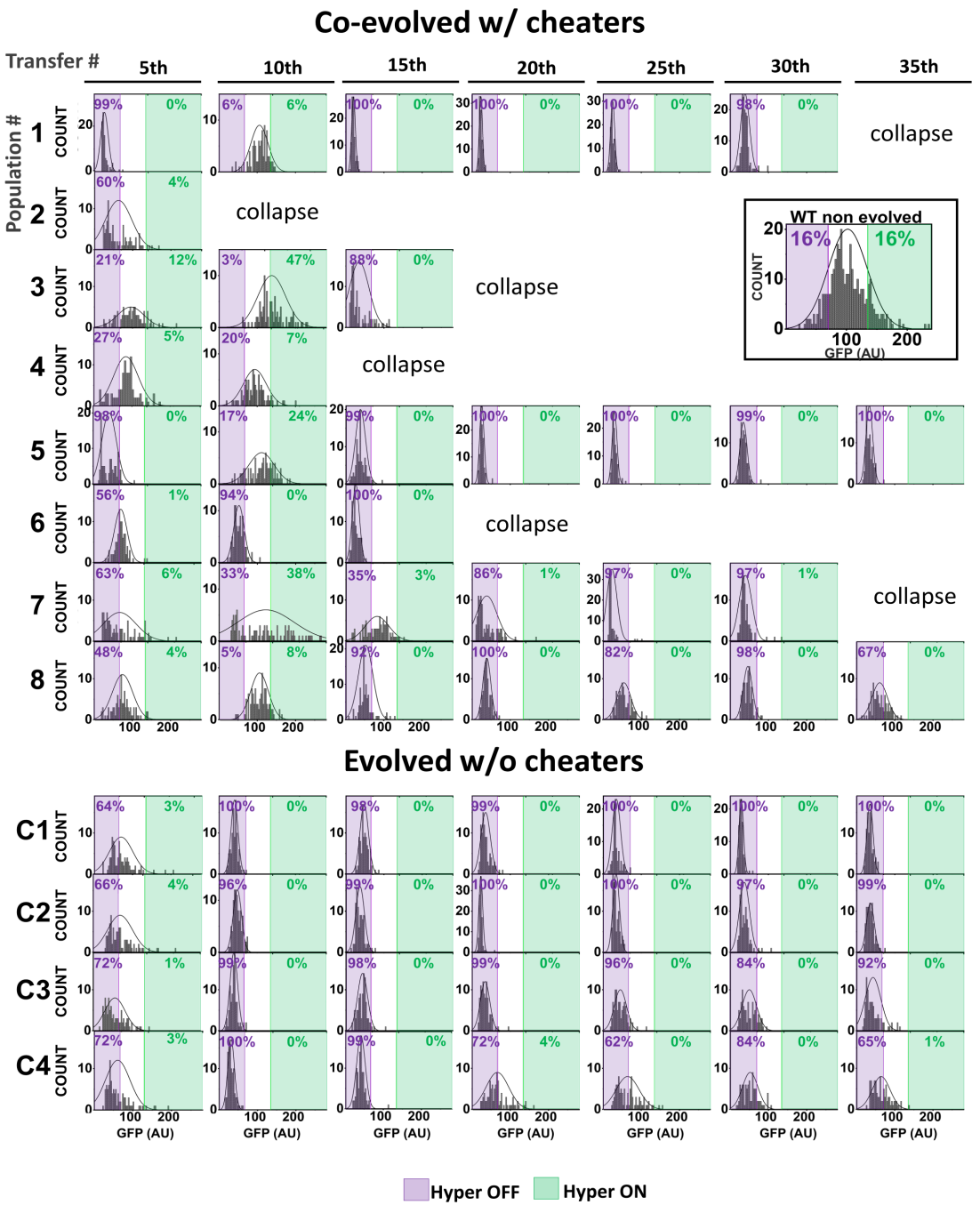
Co-evolved w/ cheaters
Transfer #
5th
10th
15th
20th
25th
30th
35th
Population #
1
2
3
4
5
6
7
8
COUNT
collapse
WT non evolved
16%
16%
GFP (AU)
Evolved w/o cheaters
C1
C2
C3
C4
Hyper OFF
Hyper ON

GFP
mKATE
Overlay
A)
Evolved w/o cheaters
5th C1
30th C1
35th C1
B)
WT ancestor
C)
ΔrsiX
D)
Evolved w/ cheaters
5th Pop 3
10th Pop 3
30th Pop 7

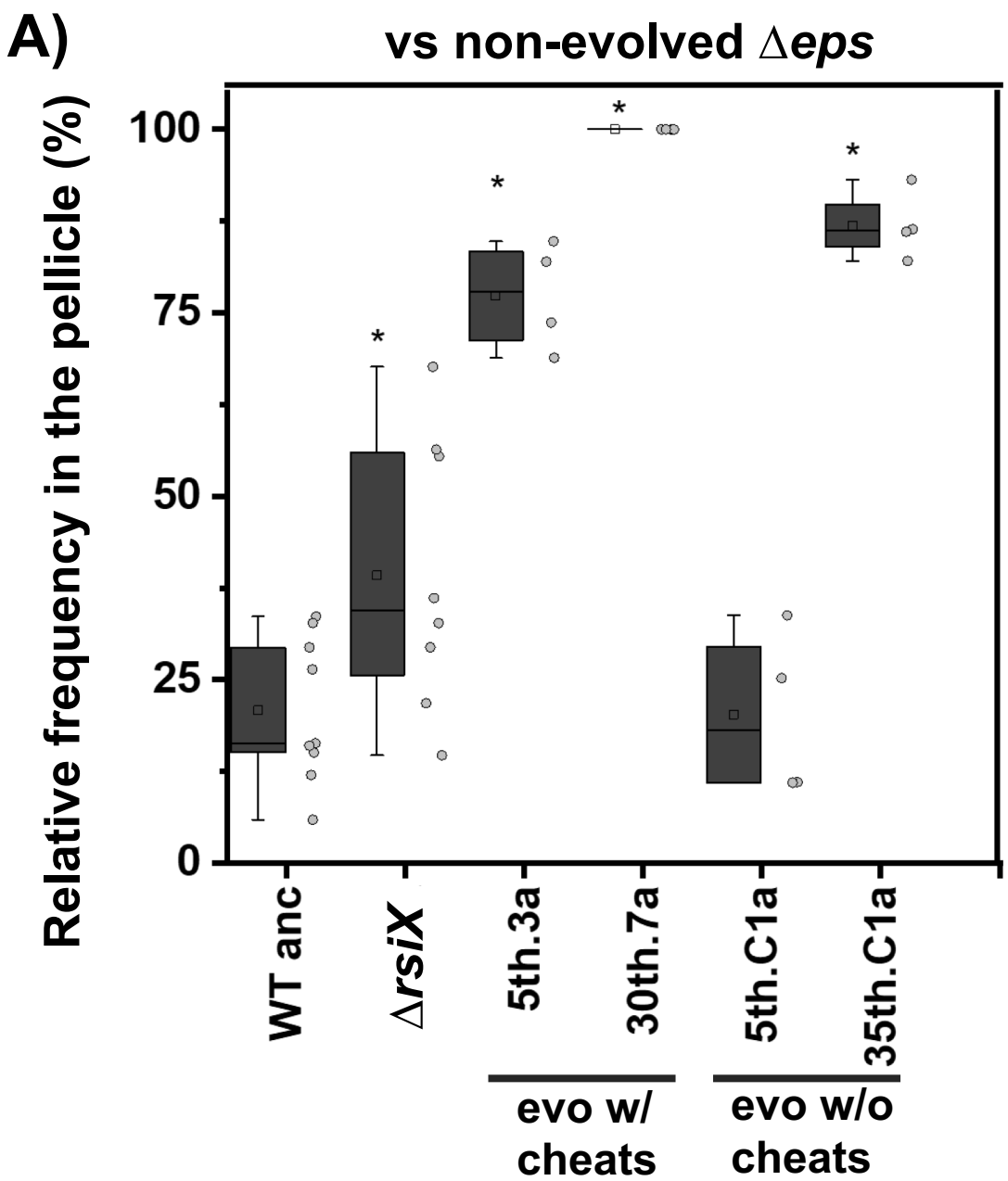
A)
vs non-evolved Δeps
Relative frequency in the pellicle (%)
100
75
50
25
0
*
*
*
*
WT anc
ΔrsiX
5th.3a
30th.7a
5th.C1a
35th.C1a
evo w/ cheats
evo w/o cheats

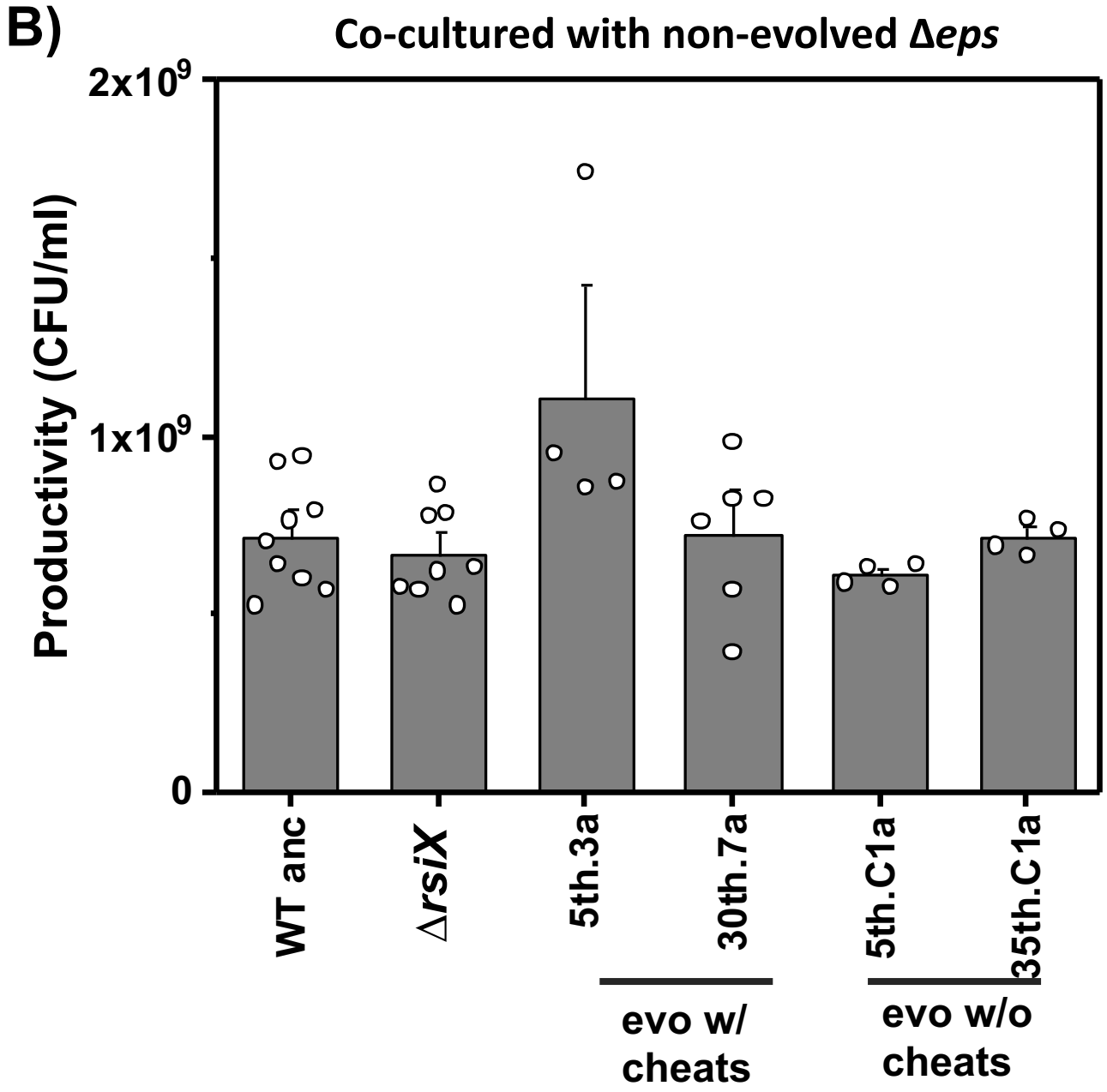
B)
Co-cultured with non-evolved Δeps
Productivity (CFU/ml)
2x10^9
1x10^9
0
WT anc
ΔrsiX
5th.3a
30th.7a
5th.C1a
35th.C1a
evo w/ cheats
evo w/o cheats

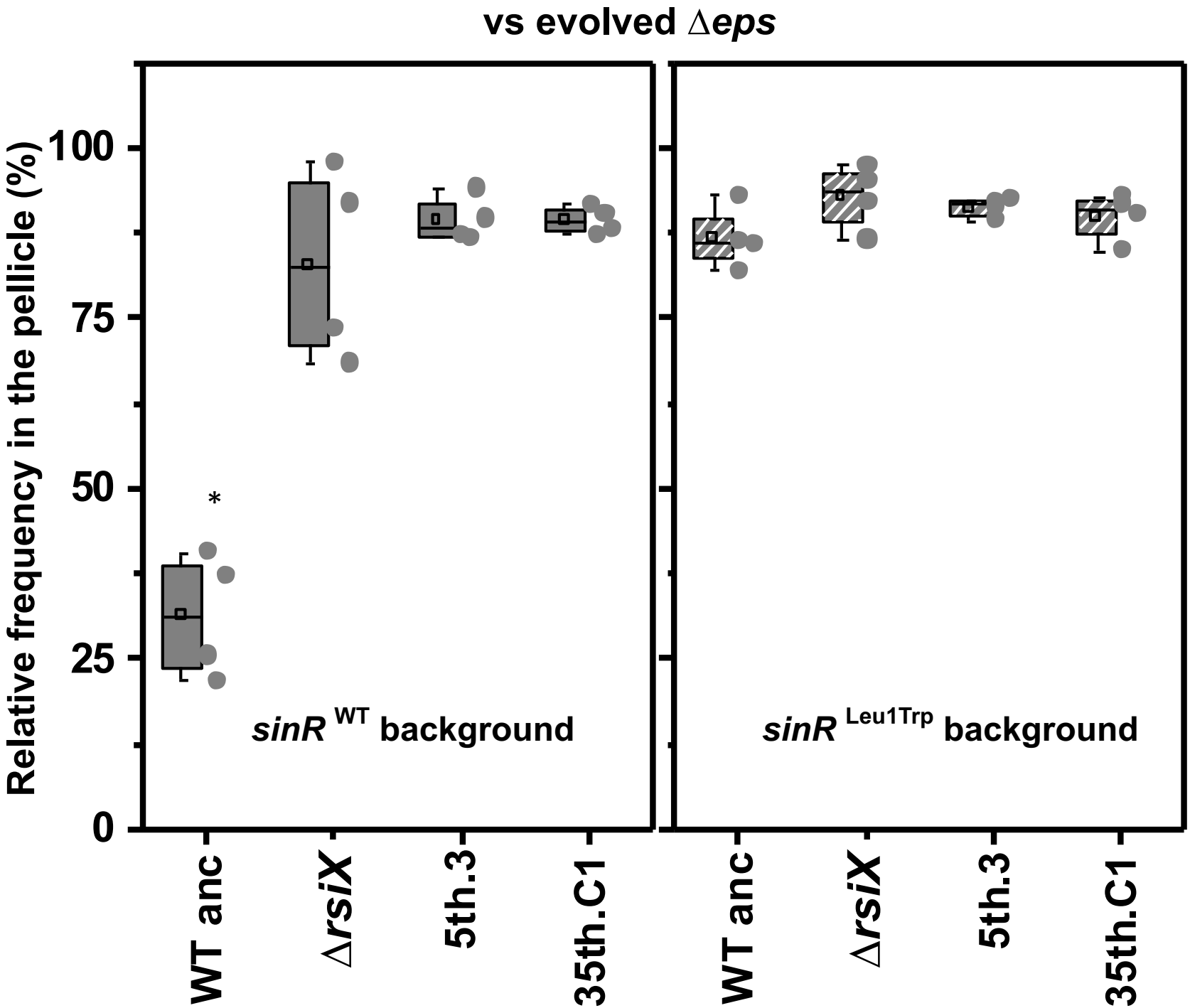
vs evolved Δeps
Relative frequency in the pellicle (%)
100
75
50
25
0
*
sinR WT background
sinR Leu1Trp background
WT anc
ΔrsiX
5th.3
35th.C1
WT anc
ΔrsiX
5th.3
35th.C1

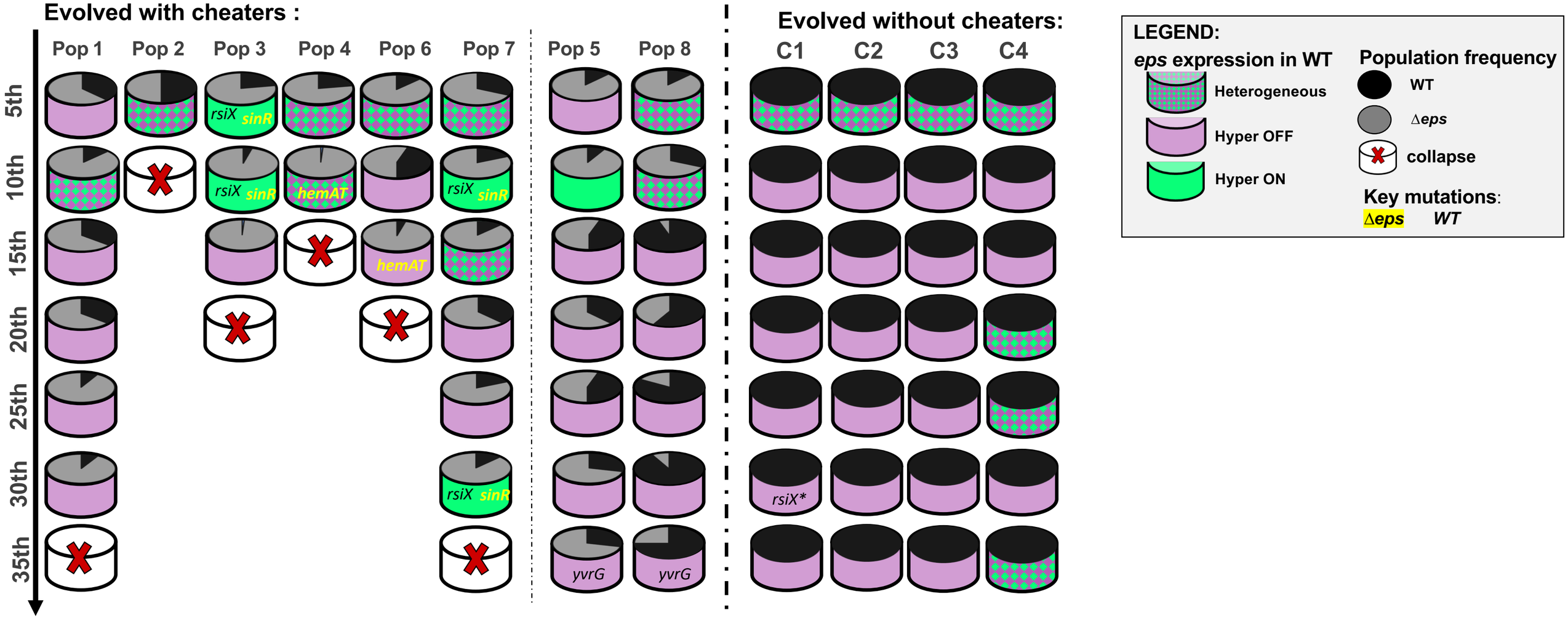
Evolved with cheaters :
Pop 1
Pop 2
Pop 3
Pop 4
Pop 6
Pop 7
Pop 5
Pop 8
5th
10th
15th
20th
25th
30th
35th
rsiX sinR
rsiX sinR
hemAT
rsiX sinR
hemAT
rsiX sinR
yvrG
yvrG
Evolved without cheaters:
C1
C2
C3
C4
rsiX*
LEGEND:
eps expression in WT
Heterogeneous
Hyper OFF
Hyper ON
Population frequency
WT
Δeps
collapse
Key mutations:
Δeps
WT